Journal of Sustainable Construction Materials and Technologies

Volume 11 | Issue 1 Article 6

2026

Impact of Glass Powder as a Sustainable Material on the Workability, Strength, and Durability Properties in High-Performance Basalt Fiber Reinforced Concrete: A Statistical Analysis

Ahmed Fathi Mohamed Salih
Department of Civil Engineering, College of Engineering, Bisha University, P.O. Box 67711, Bisha 61361, Saudi Arabia, afathi@ub.edu.sa

Recommended Citation
Salih, Ahmed Fathi Mohamed (2026) "Impact of Glass Powder as a Sustainable Material on the Workability, Strength, and Durability Properties in High-Performance Basalt Fiber Reinforced Concrete: A Statistical Analysis," *Journal of Sustainable Construction Materials and Technologies*: Vol. 11: Iss. 1, Article 6.
https://doi.org/10.29187/2458-973X.1214
Available at: https://commons.yildiz.edu.tr/jscmt/vol11/iss1/6

JOURNAL OF SUSTAINABLE CONSTRUCTION MATERIALS AND TECHNOLOGIES 2026;11:132–154

RESEARCH ARTICLE

Impact of Glass Powder as a Sustainable Material on the Workability, Strength, and Durability Properties in High-Performance Basalt Fiber Reinforced Concrete: A Statistical Analysis

Ahmed Fathi Mohamed Salih

Department of Civil Engineering, College of Engineering, Bisha University, P.O. Box 67711, Bisha 61361, Saudi Arabia

ABSTRACT

The global construction sector is increasingly challenged to balance environmental sustainability with the growing demand for durable, high-performance materials. As cement production continues to be a major source of anthropogenic CO_2 emissions, the incorporation of alternative, low-impact binders has become a key strategy for reducing the environmental footprint of concrete. In this context, glass powder (GP)—a finely ground industrial by-product rich in amorphous silica—has emerged as a promising partial replacement for Portland cement. Its pozzolanic reactivity contributes to improved hydration and matrix densification, while its use also supports circular economy principles by diverting waste glass from landfills.

At the same time, basalt fibers have attracted considerable attention as an advanced reinforcement material due to their high tensile strength, chemical stability, and thermal resistance. Their inclusion in concrete has been shown to enhance ductility, limit crack propagation, and improve overall mechanical performance. The potential synergy between glass powder and basalt fibers therefore presents an attractive opportunity to develop composite concrete systems that simultaneously address structural performance and environmental considerations.

Within this framework, the present study conducts an experimental and statistical investigation into the combined effects of GP and basalt fibers in high-performance concrete, focusing on key performance indicators including workability, compressive strength, tensile strength, flexural strength, and durability under aggressive exposure conditions. The results indicate that incorporating glass powder at selected replacement levels can lead to favorable mechanical performance, particularly when used in conjunction with basalt fibers. These findings highlight the potential of multi-component material systems to enhance the sustainability of concrete, while also underscoring the importance of considering site-specific conditions and climatic influences when optimizing mixture design.

Keywords: Glass powder, Basalt fiber, High-performance concrete, Sustainability, Strength and durability

1. Introduction

Concrete remains a cornerstone of modern infrastructure because of its wide availability, versatility, and reliable mechanical performance; nevertheless, its extensive use carries a notable environmental cost. In particular, the production of Portland cement is responsible for nearly 8% of global anthropogenic CO_2 emissions [1–3], intensifying the need for construction materials that can reduce cement demand without sacrificing structural performance. In response, recent research has increasingly explored the combined use of supplementary cementitious materials (SCMs) and advanced reinforcement strategies as practical pathways toward more sustainable and durable concrete systems.

Among the emerging SCMs, glass powder (GP), obtained from finely ground waste glass, has attracted

Received 30 October 2025; revised 16 December 2025; accepted 21 February 2026.
Available online 13 March 2026

E-mail address: afathi@ub.edu.sa (A. F. Mohamed Salih).

https://doi.org/10.29187/2458-973X.1214

growing interest due to its high amorphous silica content and pronounced pozzolanic activity. When partially replacing cement, GP reacts with calcium hydroxide to form additional calcium silicate hydrate (C–S–H), leading to a denser microstructure, refined pore network, and improved long-term mechanical behavior. Numerous studies have reported that cement replacement levels in the range of 10–20% can enhance compressive strength, reduce permeability, and simultaneously address waste management challenges by diverting non-biodegradable glass from landfills [4–6].

At the same time, fiber reinforcement has been widely investigated as an effective means of overcoming the inherent brittleness of cementitious materials. Basalt fiber (BF), derived from natural volcanic rock, is characterized by high tensile strength, chemical inertness, and thermal stability. Its inclusion in concrete has been shown to improve tensile and flexural performance, suppress microcrack development, and enhance resistance to elevated temperatures and aggressive exposure conditions, positioning BF as a viable reinforcement for high-performance concrete applications [7].

More recently, the hybrid incorporation of GP and BF has emerged as a promising strategy for achieving concurrent improvements in mechanical performance and environmental sustainability. Experimental evidence suggests that GP-induced matrix refinement can complement BF crack-bridging mechanisms, resulting in enhanced strength, toughness, and durability. For example, Xu et al. [8, 9] reported that basalt fiber–reinforced concretes containing mineral powders maintained structural integrity at temperatures approaching 600 °C, while Singh et al. [10] observed notable gains in compressive strength and ductility through optimized BF content and geometry. Additional investigations have also documented reduced water absorption and improved abrasion resistance when GP and BF are used together.

Despite these encouraging findings, comprehensive studies addressing the combined influence of GP and BF on fresh properties, mechanical behavior, and durability remain relatively limited. In particular, systematic statistical analyses of their joint effects on durability-related indicators—such as freeze–thaw resistance—are still scarce, even though these properties are closely interlinked and critically affect long-term structural serviceability [11, 12].

To bridge this gap, the present study presents an integrated experimental and analytical evaluation of concrete incorporating both glass powder and basalt fiber. The hybrid system is assessed in terms of workability, compressive strength, splitting tensile strength, flexural performance, and freeze–thaw resistance, with the objective of identifying mix designs that reconcile sustainability goals with structural performance requirements. Ultimately, the outcomes of this work aim to contribute to the development of eco-efficient, high-performance concrete suitable for future infrastructure applications.

1.1. Research objectives

This study explores the integration of finely ground recycled glass powder as a supplementary cementitious material in high-performance basalt fiber-reinforced concrete (HPBFC), with the dual objective of improving mechanical performance and promoting environmental sustainability in the construction industry. As the environmental costs of traditional concrete, which are mostly caused by too much cement consumption and industrial waste, become more and more unsustainable, using other materials like glass powder is a good and eco-friendly way to solve the problem. The research systematically investigates the influence of varying glass powder dosages on critical performance parameters, including compressive and tensile strength, fresh mix workability, and key durability indicators. HPBFC, as a composite system, is engineered to surpass traditional concrete in strength and resilience, while the inclusion of glass powder is anticipated to reduce the brittleness typically associated with high-strength concrete. In addition to looking at how well the concrete matrix works and how long it lasts, the study also looks at how the microstructure of the concrete matrix changes over time using advanced analytical methods. It focuses on how water moves through the matrix and how calcium hydroxide crystals form. These analyses yield critical insights into the physicochemical interactions between the recycled glass particles and the cementitious phase, facilitating a comprehensive knowledge of long-term performance behavior. The research is organized around three main goals: looking at how mechanical strength develops, looking at slump characteristics, and looking at durability in harsh environments. This research collectively creates a robust experimental framework validating the viability of glass powder-enhanced HPBFC in structural applications. The results contribute to the overarching quest for high-performance, low-carbon concrete solutions and underscore the significance of circular economy initiatives in sustainable construction.

2. Materials and methods

2.1. Ordinary portland cement (OPC)

In line with British standard BS 12, BS EN 197-1:2000 and ASTM C150-07, the Ordinary Portland

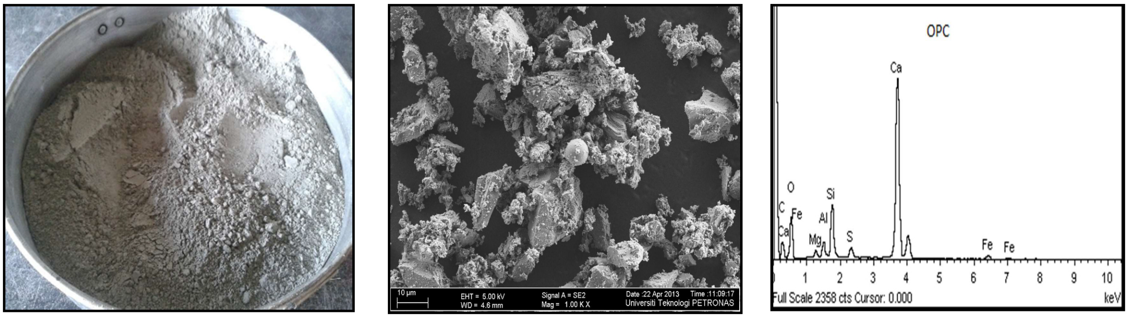

Fig. 2.1. Photo, FESEM image and XRD result of ordinary portland cement (OPC).

Cement (OPC) used in this experimental research was complied with Malaysian standard SIRIM MS 522: Part I: 2000, certificate no: PT020301. The OPC was a 50 kg weight product obtained from Tasek Corporation Berhad, Ipoh, Malaysia. The photo of OPC, FESEM photo and the XRD results are presented in Fig. 2.1. They prove that the particles of OPC show a slight variation in size and shape. The chemical and physical compositions of the OPC are presented in Tables 2.1 and 2.2.

Table 2.1. Chemical composition of the cement.

Chemical Composition	OPC
SiO_2	20.3
Al_2O_3	4.2
Fe_2O_3	3
CaO	62
MgO	2.8
SO_3	3.5
K_2O	0.9
Na_2O	0.2
LOI	2.00

Table 2.2. Physical properties of the cement.

Physical Properties	OPC
Specific gravity	3.15
Fineness (passing 45 μm)	93.10
BET surface (m^2/g)	0.6957
Adsorption average pore width (Å)	141.27

2.2. Aggregate

The fine aggregate utilized in the experiment was clean natural sand with a specific gravity of 2.61 and fineness modulus of 2.76 with a water absorption of 0.96; the maximum size was not more than 3.35 mm. The coarse aggregate utilized was (5.0 - 20) mm crushed granite stone according to BS: 812-103.2-1989 having a specific gravity of 2.66 in SSD and water absorption of 1.18. The two aggregates (Fig. 2.2) were sieved as highlighted in Graph 1.

The coarse aggregate was first sieved after which it was submerged in water and then dried for 24 hours at room temperature. The reason for immersion was to remove dirt at the top of the coarse aggregate that could have reduced the strength or proportion of the concrete, as well as to make sure that the coarse aggregate was fully saturated. Then, the coarse aggregate was dried for one more day at room temperature to make sure that the coarse aggregate's condition was saturated surface dry (SSD). The coarse aggregate used in this study was clean, hard, and strong, and was free from absorbed chemicals and clay coatings. It was sourced from a local quarry and conformed to the relevant ASTM specifications for concrete aggregates, for example:

a. Aggregate Impact Value
b. Silt content Test
c. Sieve Analysis

2.3. Basalt fiber (BF)

Basalt fiber (BF) (Fig. 2.3) is a new type of fiber that is obtained from China and is made from basalt rock. The basalt fiber is dark brown with an elastic modulus of 80-100 Gpa; the fiber length is 25.00mm with a 0.18 μm diameter and aspect ratio of 138.89. The density of the basalt fiber is 2.6-2.8 g/cm^3 and the tensile strength is 3200 MPa. At the time of mixing, it is recommended to prohibit the touching of the fibers and wear plastic gloves to prevent any itching that can be caused by this fiber.

2.4. Glass powder

Recycled glass powder that is finely powdered (20-75 μm) makes concrete stronger by reducing the amount of cement. This is because it has a pozzolanic effect. It makes things less porous and less likely to be attacked by chloride, especially when conditions are really bad. The first step in treating glass powder is to collect and process the waste glass so that

Fig. 2.2. Coarse (5.0–20 mm) and fine (< 3.35 mm) aggregates.

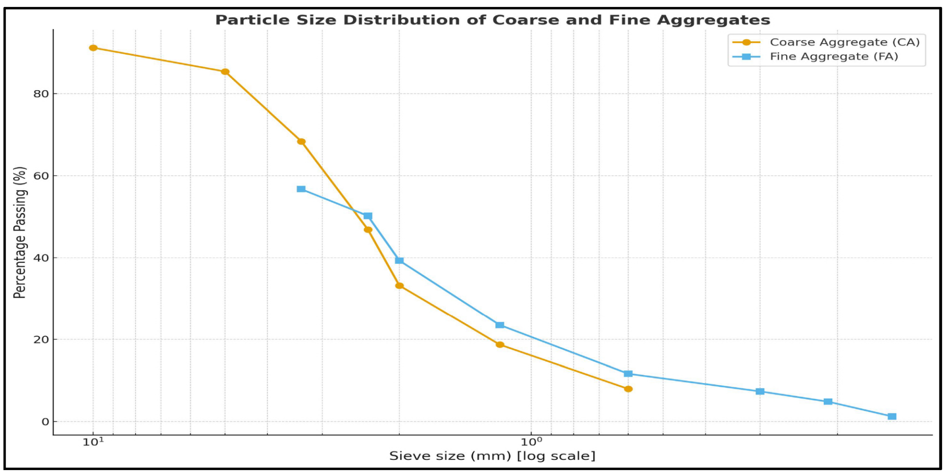

Graph 1. Practical size distribution of coarse and fine aggregate.

Figure 2.3. Basalt fiber.

metals, polymers, and ceramics that were not glass are removed. After being stored, the glass was cleaned using pure water to get rid of any dust, biological waste, or flaws on the surface. After that, it was dried so that the moisture would not get in the way of grinding. The glass was put through a ball mill after it had been dried until the particles were a fine powder with a maximum size of 75 microns, which was fine enough for pozzolanic activity. A sieve was used to make sure that all the pieces of the crushed powder were the same size. X-ray fluorescence (XRF) and X-ray diffraction (XRD) studies were used to make sure the material was safe to use. Based on the tests in Table 2.3, it possessed a lot of silica and was largely in an amorphous state. In addition to that the specific surface area (BET) of waste glass powder after it is treating found in the range of 250–600 m^2/kg. Lastly, the treated glass powder was stored in dry, sealed containers to keep it from getting wet and to maintain the same quality for its subsequent use.

2.5. Concrete mix design

Twenty-five concrete mixtures were formulated to evaluate the synergistic effects of basalt fiber and glass powder on the characteristics of high-performance concrete. The water-to-cement (W/C) ratio was meticulously controlled within the range of 0.40 to 0.43 to guarantee consistent workability and performance across all mixtures. The quantities of coarse and fine aggregates were modified within specific limits (1000–1060 kg/m^3 and 750–810 kg/m^3, respectively) to enhance particle packing and flow properties. Glass powder served as a partial cement substitute at replacement levels of 0%, 5%, 10%, 15%, and 20%, equating to GP contents from 0 to

Table 2.3. Summary of XRF and XRD results for treated glass powder.

Test	Parameter	Result	Remarks
XRF	SiO_2 (%)	> 70%	Indicates high pozzolanic potential
	$Na_2O + K_2O$ (%)	< 2%	Within safe limits to minimize ASR risk
	CaO (%)	8–12%	May contribute to hydration products
	Al_2O_3 (%)	5–8%	Enhances matrix densification
	MgO (%)	1–3%	Minor but stable content
XRD	Crystallinity	Amorphous	Broad hump at $2\theta = 20^\circ$–35°
	Pozzolanic potential	Confirmed	Amorphous phase suitable for C-S-H formation

Table 2.4. Concrete mixes.

Mix ID	Glass Powder (% of Cement)	Basalt Fiber (% by Volume)	Cement (kg/m^3)	GP (kg/m^3)	BF (kg/m^3)	Water (kg/m^3)	Sand (kg/m^3)	Coarse Aggregate (kg/m^3)	Water-Cement Ratio
N1	**0**	**0**	**400**	**0**	**0**	**160**	**800**	**1050**	**0.4**
N2	5	0.2	380	20	4.8	152	780	1030	0.4
N3	10	0.4	360	40	9.6	144	770	1020	0.4
N4	15	0.1	340	60	2.4	136	760	1010	0.4
N5	20	0.3	320	80	7.2	128	750	1000	0.4
N6	5	0.5	380	20	12	162	810	1050	0.43
N7	10	0.6	360	40	14.4	155	800	1040	0.43
N8	**15**	**0**	**340**	**60**	**0**	**136**	**790**	**1030**	**0.4**
N9	20	0.1	320	80	2.4	130	780	1020	0.41
N10	**0**	**0.2**	**400**	**0**	**4.8**	**170**	**810**	**1050**	**0.43**
N11	10	0.3	360	40	7.2	148	780	1030	0.41
N12	15	0.4	340	60	9.6	142	770	1020	0.42
N13	20	0.5	320	80	12	135	760	1010	0.42
N14	**5**	**0**	**380**	**20**	**0**	**160**	**810**	**1040**	**0.42**
N15	10	0.1	360	40	2.4	153	800	1030	0.43
N16	15	0.2	340	60	4.8	146	790	1020	0.43
N17	20	0.3	320	80	7.2	138	780	1010	0.43
N18	**0**	**0.4**	**400**	**0**	**9.6**	**172**	**810**	**1060**	**0.43**
N19	5	0.5	380	20	12	164	800	1050	0.43
N20	10	0.6	360	40	14.4	156	790	1040	0.43
N21	**15**	**0**	**340**	**60**	**0**	**136**	**770**	**1020**	**0.4**
N22	20	0.1	320	80	2.4	128	760	1010	0.4
N23	10	0.4	360	40	9.6	150	780	1040	0.42
N24	15	0.5	340	60	12	142	770	1030	0.42
N25	20	0.6	320	80	14.4	136	760	1020	0.43

80 kg/m^3. Basalt fiber was added ranging from 0% to 0.6% by volume (0–14.4 kg/m^3) and was incorporated to enable a comprehensive analysis of its impact on the tensile and flexural properties. Specific mixtures were created to isolate the individual effects of each additive (e.g., GP only, BF only), while others assessed their combined impact. Table 2.4 shows the details of 25 concrete mix designs, highlighting differences in the water-cement ratio, aggregate proportions, cement content, and the amounts of basalt fiber and glass powder used in each mix.

The mix proportions in Table 2.4 were determined based on EN 206 mix design guidelines, targeting high-performance concrete with suitable slump and strength. Adjustments were made to accommodate basalt fibers and glass powder, and proportions were refined through preliminary trial mixes to ensure homogeneous and practical mixes.

In this study, the concrete is considered high-performance, with a 28-day characteristic compressive strength of 40 MPa. The mix design follows the European Standard (EN 206), incorporating necessary modifications to accommodate basalt fibers and glass powder as supplementary materials. This approach ensures that the concrete achieves the required strength and durability for high-performance applications while conforming to established design standards.

3. Literature review

This review integrates contemporary research across five thematic domains to build a foundational framework for the current study and to rigorously pinpoint knowledge deficiencies.

It focuses on the performance of concrete modified with ground glass powder (GP) and basalt fiber (BF), evaluating their respective and combined influences on workability, mechanical behavior, durability, and microstructural characteristics. Special attention is paid to the role of GP in enhancing the matrix chemistry and sustainability, and to BF in strengthening the tensile and fracture resistance properties of concrete composites. The insights provided here position GP-BF hybrid systems as a forward-looking solution aligned with both performance and environmental objectives.

3.1. Integration of glass powder and basalt fiber in concrete

Glass powder (GP) contributes to enhanced hydration and a denser matrix when it replaces 20–30% of cement, leading to improved strength and durability, though ASR mitigation through supplementary materials remains necessary [13, 14]. Basalt fiber (BF), offering tensile strengths up to 4840 MPa, strengthens flexural performance and helps limit cracking at dosages under 0.5%; however, higher amounts tend to cause fiber clumping and hinder workability, underscoring the importance of carefully optimized mix proportions.

When GP and BF are incorporated together, they yield complementary benefits, such as stronger interfacial bonding, reduced microcracking, and marked improvements in abrasion resistance and energy absorption. Although BF is vulnerable to long-term alkaline degradation, it still performs better than glass and carbon fibers under aggressive conditions. Overall, the GP–BF combination presents a promising, sustainable enhancement for concrete, well-suited to advanced construction technologies including 3D printing [15–22].

3.2. Fresh-state behavior: Influence of glass powder and basalt fiber on slump characteristics

GP typically improves the flowability of concrete by lowering internal friction and promoting better particle dispersion, with a 20% replacement level capable of increasing slump flow by as much as 22%. Conversely, BF sharply reduces slump—by up to 78% at a 1.5% volume fraction—because of its geometry and surface texture, which requires increased superplasticizer use to maintain workable consistency [23–26].

Even so, hybrid mixtures such as 10% GP combined with BF can still satisfy EN 206-1 flow criteria, while appropriate GP fineness and admixture adjustments help keep slump flow within SCC standards. Rheological behavior is further affected by aggregate characteristics and temperature, highlighting the need for carefully managed admixture strategies in BF-reinforced concrete systems [27–33].

3.3. Mechanical properties: Strength characteristics of GP and BF modified concrete

GP increases compressive strength by enhancing matrix packing and promoting secondary hydration, with strength gains of 18–22% documented in fiber-reinforced mixtures. BF further improves toughness and crack resistance, while hybrid blends containing 20% GP and 0.2% BF can deliver strength increases of up to 25% due to a more refined pore network and stronger ITZ cohesion [34–37].

In UHPC, BF contents of 0.75–1% can achieve compressive strengths exceeding 85 MPa and maintain performance after thermal exposure. Predictive modeling tools also help refine GP–BF mixture designs, lowering embodied carbon by as much as 35% and enabling the large-scale reuse of waste glass in sustainable concrete applications [38, 39].

3.4. Durability performance: Resistance to environmental degradation

BF markedly enhances durability by limiting chloride penetration and improving freeze–thaw performance, cutting ionic transport by 40% and doubling resistance to freeze–thaw cycles at low fiber contents. GP strengthens this effect by refining the pore structure, while hybrid GP–BF mixtures can reduce mass loss by up to 60% after 300 cycles. Field evidence further supports BF's role in improving UHPC durability and in strengthening retrofitted structures [40–49].

Microstructural studies indicate that GP produces denser hydration products, whereas BF disrupts capillary channels, resulting in a 45% reduction in pores larger than 100 nm and a 25% decrease in ITZ porosity. Substituting sand with GP can raise strength by 18%, and combining multiple fiber types helps better control pore gradation, establishing GP–BF concrete as a resilient, thermally stable, and sustainable material choice [50–55].

4. Scope and significance

This study aims to develop, refine the strength performance of high-strength, high-performance basalt fiber concrete (BFC) incorporating ground glass powder (GP) as a partial cement substitute. The concrete mixtures analyzed are produced using controlled molding techniques and defined curing regimes. The core research question guiding this work is: Can the mechanical performance of sustainable BFC mixtures enhanced with mineral admixtures and structured through advanced mix dispersion series be reliably predicted using statistical design methods. To address this, a subsidiary question is posed: How do the individual effects of casting and compaction influence the different parameter on workability, strength, and crack resistance behavior.

The investigation focuses specifically on mechanical response variables relevant to high-performance BFC with GP admixture, rather than attempting to generalize across the entire field of concrete materials science. Its main contribution is that it models the many interactions between the different parts of a mixture during dispersion and molding, and it quantifies how those interactions affect strength development.

The study also shows how useful recycled glass may be as a raw material for future cementitious composites, especially as it comes in a variety of chemical grades. If this resource is well-integrated into regional construction programs, it might boost local economies by creating jobs, encouraging entrepreneurship, and adding value through new ways to use materials. The broader significance of this work lies in its potential to inform cost-effective, sustainable infrastructure solutions for post-crisis reconstruction and public works through the deployment of high-performance, low-carbon building materials.

5. Ground glass powder in concrete: Production, properties, and performance

Recycled glass powder (RGP), synthesized through advanced comminution of discarded glass products (predominantly soda-lime variants), has gained prominence as an innovative supplementary cementitious material (SCM) for sustainable concrete production. The production protocol includes stages for decontamination, fragmentation, and pulverization, which produce particles smaller than 75 μm. The fractions less than 20 μm are more reactive.

Characterized by a silica-rich amorphous phase ($\geq$70% SiO_2), RGP engages in pozzolanic interactions with portlandite during hydration, generating supplementary calcium silicate hydrate (C-S-H) phases that refine the pore structure and amplify the mechanical performance over extended curing periods [56, 57].

Strategic substitution of 10–30% Portland cement with RGP confers multifaceted engineering and ecological benefits. Beyond augmenting structural resilience through diminished permeability and fortified resistance to ionic penetration (e.g., sulfates, chlorides), optimized RGP formulations effectively suppress deleterious alkali-silica reactions (ASR) via silica-alkali binding mechanisms. From an environmental perspective, RGP deployment directly addresses anthropogenic waste streams by repurposing landfill-destined glass while curtailing clinker production—a critical lever for decarbonizing the construction sector. Notably, RGP-modified composites exhibit enhanced rheological properties in architectural concrete, enabling precise surface finishes without compromising bulk integrity [58–60].

However, material limitations warrant judicious formulation protocols. Dosages exceeding 30% risk reintroducing ASR susceptibility, particularly when processing inadequately homogenized glass feedstocks with fluctuating alkali profiles. Early-age strength retardation, attributable to delayed pozzolanic kinetics, remains a concern unless ultrafine particle gradations (<10 μm) are achieved. Furthermore, compositional heterogeneity across waste sources necessitates robust feedstock characterization and real-time quality monitoring to ensure batch consistency. Paradoxically, while RGP's chemical variability poses formulation challenges, it simultaneously highlights its versatility in regionally tailored applications where local waste streams can be leveraged. When integrated within circular economy frameworks, RGP-engineered concretes exemplify the symbiosis between infrastructure durability and resource stewardship a critical advancement as global urbanization intensifies demand for low-embodied-carbon building solutions.

6. Mechanical and structural role of basalt fiber in high-performance concrete

Basalt fiber-reinforced concrete (BFRC), an engineered composite synthesized by strategically incorporating volcanic basalt rock-derived filaments into cementitious matrices, represents a paradigm shift in high-performance construction materials. These fibers produced via molten rock extrusion, fiberization, and thermal stabilization are typically introduced as discrete elements (0.1–3 cm lengths) at 2–7 vol%, optimizing interfacial bonding while preserving workability. Functioning as micro-scale reinforcement, the fibers mitigate crack propagation through stress redistribution, concurrently elevating tensile capacity (2.6–4.8 GPa), flexural toughness, and impact resilience. Their intrinsic thermal inertness (serviceable to 750°C) and electrochemical stability position them as ideal candidates for infrastructure subjected to cyclic thermal gradients, marine environments, or dynamic loading regimes [61, 62].

BFRC fundamentally redefines concrete's failure mechanics, transitioning brittle fracture patterns to progressive, energy-dissipative modes. While compressive strengths align with high-performance concrete benchmarks (60–120 MPa), the material's distinction lies in its post-crack ductility a property arising from synergistic fiber-matrix interactions that homogenize strain distribution and dissipate fracture energy through controlled fiber pull-out mechanisms. This pseudo-ductile behavior proves critical in applications demanding vibration damping, blast resistance, or fatigue endurance, with documented performance enhancements in bridge decks, seismic retrofits, and Arctic infrastructure where freeze-thaw cycling compromises conventional concretes.

From a sustainability perspective, BFRC addresses dual priorities: structural resilience and ecological stewardship. Basalt fiber production requires 30–50% less energy than synthetic alternatives (e.g., carbon/glass fibers), leverages Earth's most abundant igneous resource, and generates no toxic byproducts. Recent lifecycle analyses reveal that coupling BFRC with industrial byproducts like metakaolin or recycled glass powder amplifies durability while reducing the mix's embodied carbon by up to 40%—a synergy aligning with circular economy principles [63–65]. Notably, the material's compatibility with automated construction techniques, such as 3D concrete printing, underscores its role in modernizing sustainable infrastructure. As urbanization intensifies pressure on aging systems, BFRC emerges as a linchpin material, reconciling the escalating demands for disaster-resilient structures with decarbonization imperatives in the built environment.

7. Experimental design and evaluation protocol

This section outlines the comprehensive experimental framework adopted to investigate the performance of 25 engineered high-performance basalt fiber-reinforced concrete (HP-BFRC) mixtures incorporating glass powder (GP) as a sustainable alternative to ordinary Portland cement (OPC) (Fig. 7). The mix design strategy employed a systematic partial replacement of OPC by mass, ranging from 25% to 45%, with ultrafine GP (<20 μm), combined with basalt fiber volumes between 4% and 6%, to optimize both mechanical efficacy and environmental impact. A factorial matrix guided the formulation process, integrating five levels of GP substitution (25%, 30%, 35%, 40%, 45%) with five corresponding fiber dosages (4%, 4.5%, 5%, 5.5%, 6%) to enable detailed analysis of both the main and the interaction effects.

To ensure homogeneous dispersion and minimize segregation risks, GP was pre-mixed with fine and coarse aggregates before cement addition, while basalt fibers were introduced gradually under controlled shear mixing to prevent clumping. The fine GP particles served a dual function, acting as a pozzolanic agent and enhancing the fiber matrix interface by improving mix fluidity and fiber alignment. This approach was specifically calibrated to balance fresh-state stability with long-term structural integrity.

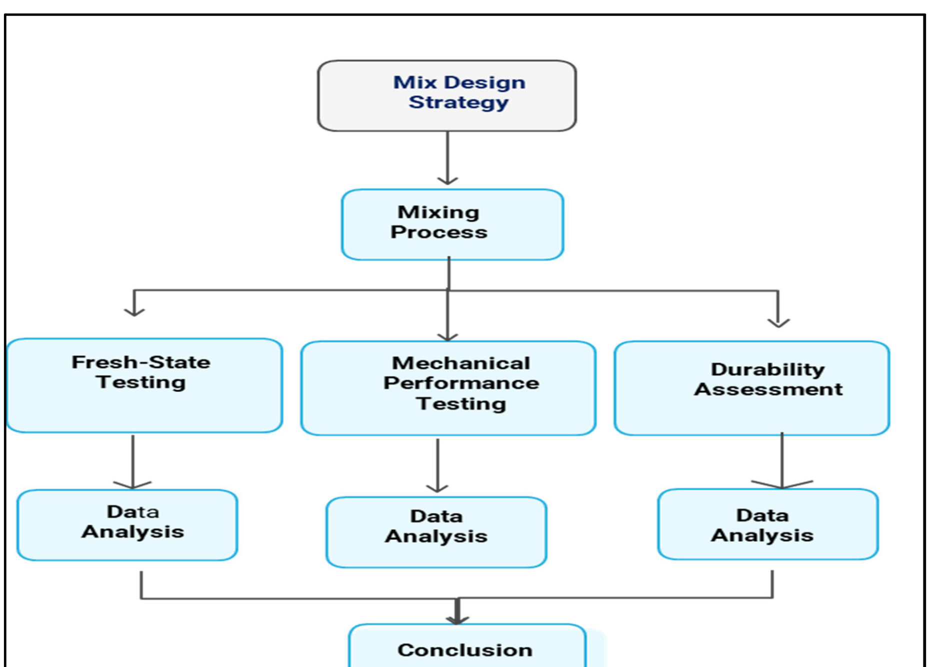

Figure 7. Experimental framework for HP-BFRC mixture.

Each of the 25 formulations underwent a multi-phase testing regime. Fresh-state behavior was evaluated through slump flow measurements to assess workability. Mechanical performance was characterized through compressive strength testing of 100 mm cube specimens of 28-days, along with the 28-day tensile strength using ASTM C496 (split-cylinder method) and flexural strength via ASTM C78 (third-point loading on 100 × 100 × 400 mm prisms). Finally, the durability was assessed using rapid chloride ion permeability (ASTM C1202) and freeze-thaw resistance, quantified as the percentage of strength retained after 300 cycles in accordance with ASTM C666. This experimental design not only ensures reproducibility but also provides a robust dataset for evaluating the synergy between GP and basalt fibers in advancing sustainable, high-performance concrete systems.

8. Results

8.1. Data description

This study evaluated five key performance properties of concrete mixes: freeze-thaw resistance, compressive strength, flexural strength, tensile strength, and slump. These properties were assessed using box plots (Fig. 8.1) alongside summary statistics (Table 8.1). Freeze-thaw resistance exhibited high durability, with a median of around 89% and a narrow interquartile range. The mean value stood at 89.16%, with a standard deviation of 3.45%, reflecting stable performance under cyclic environmental exposure. Compressive strength showed a median of approximately 46 MPa and ranged from just below 40 MPa to slightly above 52 MPa. The average value was 45.76 MPa, highlighting the overall strength quality across the mixes.

Flexural strength, with a median near 9.8 MPa and values between 8.5 and 11 MPa, demonstrated dependable resistance to bending. Similarly, tensile strength ranged from 2.8 MPa to 3.8 MPa, with a mean of 3.34 MPa and standard deviation of 0.35 MPa, reflecting moderate variation in tensile behavior. In contrast, the slump measurements, which indicate workability, showed the broadest spread among all properties. Values ranged from 50 mm to 85 mm, with a mean of 71.16 mm and a relatively high standard deviation of 9.85 mm. This variation likely results from differences in the proportions of BF and GP used across the mixtures.

8.2. Statistical analysis section

Given that glass powder (GP) and basalt fiber (BF) contents varied simultaneously and quantitatively across mixtures, a multivariable general linear modeling approach was adopted. GP and BF were treated as continuous predictors, and their interaction term was included to assess combined effects. The water–cement ratio was incorporated as a covariate to control its known influence on fresh, mechanical, and durability properties. In this way we avoid confounding inherent in one-way analyses and provide adjusted estimates of the independent and interactive effects of GP and BF

8.3. Assessment of compressive strength

The statistical analysis indicates that the proposed model explains most of the variation in 28-day compressive strength (Tables 8.3.1 and 8.3.2), with glass powder (GP) identified as the primary and statistically significant influencing factor. This observation aligns with previous studies reporting that finely ground glass powder enhances compressive strength by refining the pore structure and densifying the cementitious matrix when used within suitable replacement ranges [66]. In contrast, basalt fiber (BF) and the water-to-cement ratio do not show statistically significant independent effects on compressive strength, which is consistent with earlier findings that BF mainly contributes to improvements in tensile and flexural performance rather than compressive behavior [67].

The GP×BF interaction displays a limited, near-significant effect, suggesting a modest synergistic influence that may become more evident under alternative mix proportions or with an expanded dataset. Similar interpretations have been reported in the literature, indicating that the mechanical response of glass powder–modified concrete is primarily governed by matrix refinement and particle packing, while fiber contributions tend to play a secondary role and may be restricted by workability limitations at higher dosages [68, 69]. Overall, these results confirm that improvements in compressive strength are largely driven by GP incorporation, without evidence of adverse effects associated with BF addition or their combined use.

The diagnostic plots show a strong agreement between the observed and predicted compressive strength values at 28 days, indicating that the regression model satisfactorily represents the mechanical behavior of concrete mixtures incorporating glass powder (GP) and basalt fiber (BF) (Fig. 8.3). This agreement suggests that the contribution of GP to matrix densification and microstructural refinement has been effectively captured, which is consistent with previous findings reporting improved hydration behavior and pore

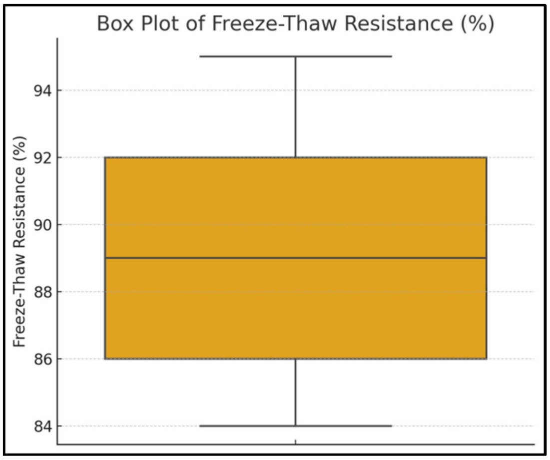

(a)

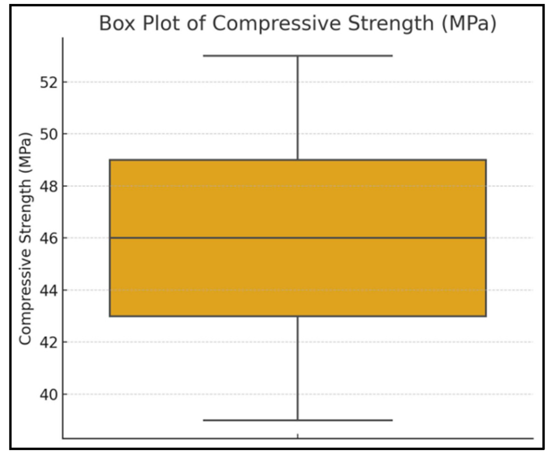

(b)

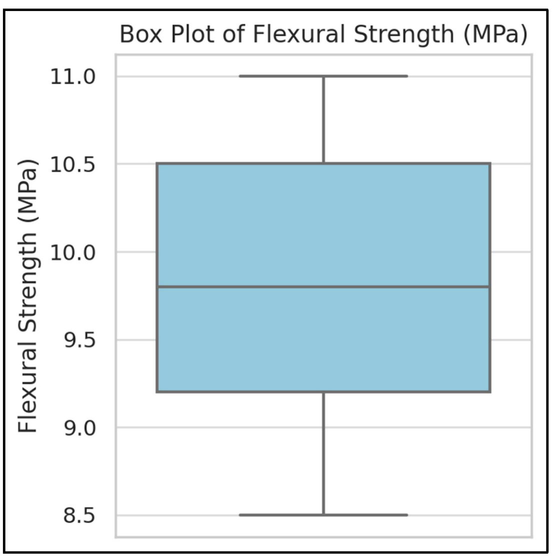

(c)

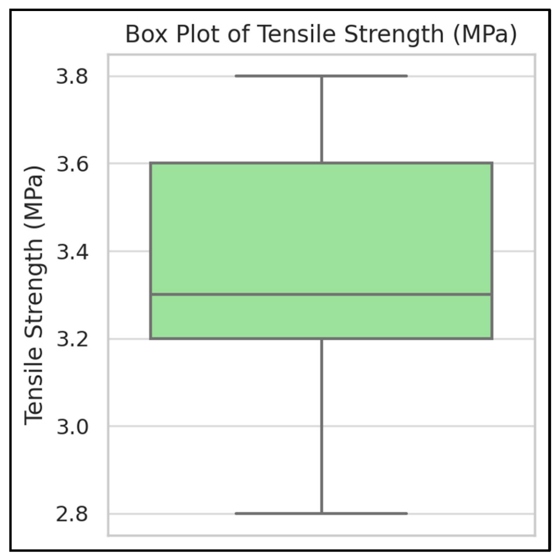

(d)

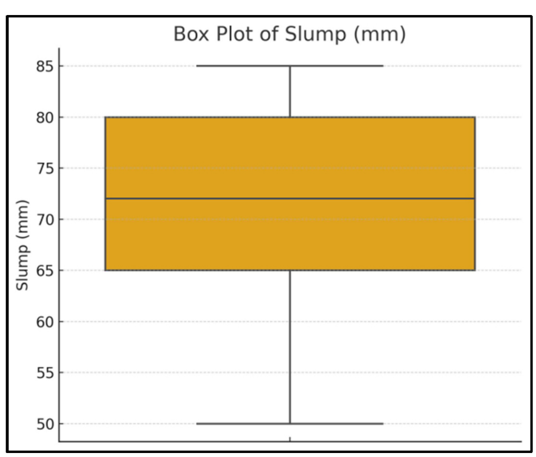

(e)

Figure 8.1. Box plot of five key parameters.

Table 8.1. Descriptive statistics of different performance properties.

Statistic	Compressive Strength (28 Days) (MPa)	Freeze-Thaw Resistance (% Retained)	Slump (mm)	Flexural Strength (MPa)	Tensile Strength (MPa)
Mean	45.76	89.16	71.16	9.84	3.34
Standard Deviation	4.11	3.45	9.85	0.75	0.35
Minimum	39.00	84.00	50.00	8.50	2.80
25th Percentile	43.00	86.00	65.00	9.20	3.20
Median (50th %)	46.00	89.00	72.00	9.80	3.30
75th Percentile	49.00	92.00	80.00	10.50	3.60
Maximum	53.00	95.00	85.00	11.00	3.80

Table 8.3.1. Tests of between-subjects effects on the 28 days compressive strength.

Source	Type III Sum of Squares	df	Mean Square	F	Sig.	Partial Eta Squared
Corrected Model	375.187[a]	4	93.797	63.867	0.000	0.927
Intercept	36.564	1	36.564	24.896	0.000	0.555
GP	81.187	1	81.187	55.281	0 .000	0.734
BF	0.317	1	0.317	0.216	0.647	0.011
W/C Ratio	1.434	1	1.434	0.977	0.335	0.047
GP * BF	4.966	1	4.966	3.381	0.081	0.145

R squared = 0 .927. Adj R sq = 0.913.

Table 8.3.2. Regression coefficients of GP, BF, W/C and GP*BF on 28 days compressive strength.

					95% Confidence Interval	
Parameter	B	Std. Error	t	Sig.	Lower Bound	Upper Bound
Intercept	49.261	9.873	4.990	0.000	28.667	69.855
GP	0.118	0.016	7.435	0.000	0.085	0.152
BF	–0.051	0.111	–0.465	0.647	–0.282	0.179
W/C Ratio	–23.633	23.913	–0.988	0.335	–73.514	26.248
GP * BF	0.004	0.002	1.839	0.081	0.000	0.008

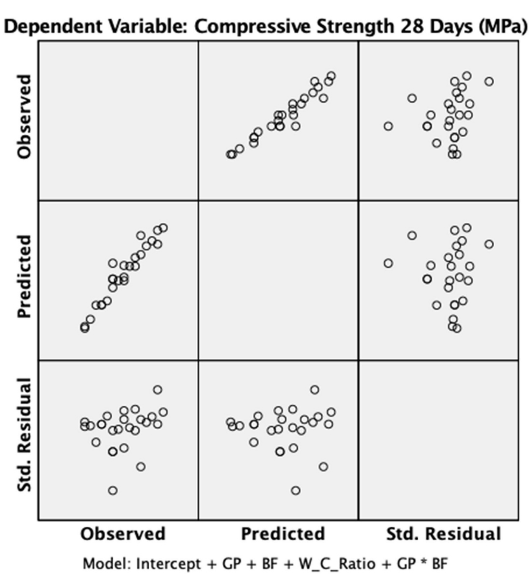

Figure 8.3. Diagnostic plot of model assumptions for compressive strength.

structure refinement in glass powder–blended cementitious systems [70]. In parallel, the stabilizing role of basalt fibers in enhancing stress transfer and controlling microcrack development supports the overall predictive performance of the model [71].

Moreover, the nearly random distribution of standardized residuals around zero, without observable trends or heteroscedastic patterns, confirms the validity of the linearity and constant variance assumptions, even with the inclusion of the GP×BF interaction term. This behavior indicates that the synergistic interaction between fine mineral admixtures and fibers has been appropriately accounted for, reducing systematic prediction errors. Similar synergistic effects have been reported in recent studies, where the combined use of mineral additives and fibers was shown to enhance mechanical consistency and limit result dispersion in concrete composites [72] Accordingly, the proposed model can be considered reliable for interpreting and predicting compressive strength in GP–BF concrete mixtures within the investigated parameter range.

8.4. Assessment of Freeze-Thaw resistance

The statistical analysis indicates that the proposed model captures freeze–thaw resistance behavior with a high level of significance ($p < 0.001$) and strong explanatory capability ($R^2 = 0.869$) (Tables 8.4.1 and 8.4.2). Glass powder

Table 8.4.1. Tests of between-subjects effects of GP, BF, W/C ratio on Freeze-Thaw resistance.

Source	Type III Sum of Squares	df	Mean Square	F	Sig.	Partial Eta Squared
Corrected Model	0.025[a]	4	0.006	33.100	0.000	0.869
Intercept	0.015	1	0.015	81.235	0.000	0.802
GP	0.009	1	0.009	48.069	0.000	0.706
BF	7.287E-5	1	7.287E-5	0.389	0.540	0.019
W_C_Ratio	0.000	1	0.000	1.859	0.188	0.085
GP * BF	0.000	1	0.000	2.624	0.121	0.116

R Squared = 0.869 (Adjusted R Squared = 0.843).

Table 8.4.2. Regression coefficients of GP, BF, W/C and GP*BF on Freez-Thaw resistance.

Parameter	B	Std. Error	t	Sig.	95% Confidence Interval	
					Lower Bound	Upper Bound
Intercept	1.005	0.111	9.013	.000	0.772	1.237
GP	0.001	0.000	6.933	.000	0.001	0.002
BF	–0.001	0.001	–0.624	.540	–0.003	0.002
W_C_Ratio	–0.368	0.270	–1.364	.188	–0.931	0.195
GP * BF	–3.658E-5	2.258E-5	–1.620	.121	–8.369E-5	1.053E-5

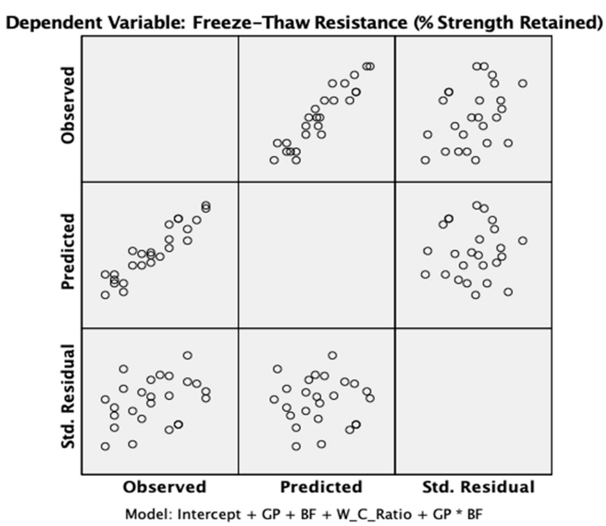

Figure 8.4. Diagnostic plot of model assumptions for Freeze-Thaw resistance.

(GP) emerges as the principal and statistically significant factor, which is consistent with previous studies demonstrating that GP enhances freeze–thaw durability through pore refinement and reduced permeability [52, 70]. By contrast, basalt fiber (BF) and the water-to-cement ratio do not display significant independent effects, supporting earlier observations that fiber contributions to freeze–thaw performance are generally secondary and strongly influenced by overall mixture balance [67].

The GP×BF interaction exhibits only a limited, near-significant influence, pointing to a modest synergistic effect that may become more apparent under alternative mix proportions or extended exposure conditions. Overall, these findings confirm that improvements in freeze–thaw resistance are primarily governed by GP incorporation, with no evidence of adverse effects associated with BF addition or from their combined use [73].

The diagnostic plots show a satisfactory agreement between observed and predicted freeze–thaw resistance values (% strength retained), indicating that the regression model adequately represents the durability behavior of concrete mixtures incorporating glass powder (GP) and basalt fiber (BF) (Fig. 8.4). This correspondence suggests that the role of GP in refining the pore structure and reducing water absorption has been effectively captured, which is known to enhance freeze–thaw resistance by limiting moisture ingress and internal microcracking [70]. In addition, the incorporation of BF contributes to improved crack control and stress redistribution under cyclic freezing and thawing, supporting the model's predictive performance across the investigated parameter range [71].

Furthermore, the standardized residuals are randomly distributed around zero, with no evident trends or variance amplification, confirming the validity of the linearity and homoscedasticity assumptions, even with the inclusion of the GP×BF interaction term. This statistical behavior indicates that the combined effect of GP-induced matrix densification and BF-driven crack-bridging mechanisms has been reasonably accounted for, thereby minimizing systematic prediction errors. Consequently, the proposed model can be considered reliable for interpreting and predicting freeze–thaw performance of GP–BF concrete mixtures within the studied domain.

8.5. Assessment of slump properties

The multivariable statistical modeling approach results show that the proposed model accounts for

Table 8.5.1. Tests of between-subjects effects of GP, BF, W/C ratio on slump.

Source	Type III Sum of Squares	df	Mean Square	F	Sig.	Partial Eta Squared
Corrected Model	2217.698[a]	4	554.425	101.115	0.000	0.953
Intercept	244.840	1	244.840	44.654	0.000	0.691
GP	27.157	1	27.157	4.953	0.038	0.198
BF	205.704	1	205.704	37.516	0.000	0.652
W/C Ratio	25.411	1	25.411	4.634	0.044	0.188
GP * BF	20.953	1	20.953	3.821	0.065	0.160

a. R Squared = 0.953 (Adjusted R Squared = 0.943).

Table 8.5.2. Regression coefficients of GP, BF, W/C and GP*BF on slump.

					95% Confidence Interval	
Parameter	B	Std. Error	t	Sig.	Lower Bound	Upper Bound
Intercept	127.473	19.076	6.682	0.000	87.681	167.265
GP	–0.069	0.031	–2.226	0.038	–0.133	–0.004
BF	–1.310	0.214	–6.125	0.000	–1.756	–0.864
W/C Ratio	–99.468	46.204	–2.153	0.044	–195.848	–3.088
GP * BF	–0.008	0.004	–1.955	0.065	–0.016	0.001

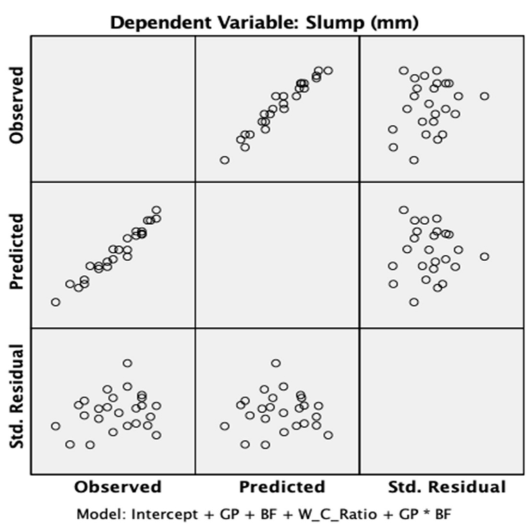

Figure 8.5. Diagnostic plot of model assumptions for slump.

nearly all the variability in slump values ($R^2 = 0.953$), highlighting the strong influence of mixture parameters on concrete workability (Tables 8.5.1 and 8.5.2). Basalt fiber (BF) exhibits the most pronounced negative effect on slump, in agreement with earlier studies indicating that fiber incorporation reduces workability as a result of increased internal friction and surface area in the fresh mixture [74, 75]. Glass powder (GP) and the water-to-cement ratio also display statistically significant, though less dominant, effects, reflecting modifications in particle packing and paste rheology associated with fine mineral additions [19].

The GP×BF interaction approaches statistical significance, suggesting a limited combined influence that may further reduce workability when both constituents are introduced simultaneously. Similar trends have been documented in the literature, where the concurrent use of mineral admixtures and fibers requires careful proportioning and fresh-state adjustments to ensure adequate flowability [76]. Overall, these findings indicate that although GP and BF contribute positively to hardened properties, their combined use demands deliberate mix design control to maintain acceptable workability.

The diagnostic plots indicate a good agreement between the observed and predicted slump values, suggesting that the regression model adequately captures the workability behavior of concrete mixtures incorporating glass powder (GP) and basalt fiber (BF) (Fig. 8.5). This agreement reflects the influence of GP on modifying particle size distribution and paste rheology, which can enhance flowability at moderate replacement levels by improving packing density and reducing internal friction [66]. The near-linear correspondence further indicates that the combined effects of GP content and water–cement ratio on slump have been consistently represented within the investigated mix design range.

Moreover, the standardized residuals are randomly distributed around zero without discernible trends or variance escalation, confirming the validity of the linearity and homoscedasticity assumptions, even with the inclusion of the GP×BF interaction term. This behavior suggests that the reduction in workability typically associated with fiber addition—due to increased surface area and fiber interlocking—has been appropriately captured by the model [67]. Accordingly, the proposed model can be considered statistically reliable for interpreting and predicting slump of GP–BF concrete mixtures within the studied parameter domain.

8.6. Assessment of tensile strength

The multivariable statistical modeling approach results show that the proposed model accounts for a considerable share of the variation in tensile strength ($R^2 = 0.755$), with glass powder (GP) and basalt fiber (BF) emerging as statistically significant contributors (Tables 8.6.1 and 8.6.2). The beneficial influence of GP is consistent with earlier studies indicating that finely ground glass powder enhances tensile performance by improving matrix continuity and strengthening the paste–aggregate interface [67, 78]. Likewise, the significant role of BF agrees with well-established findings that basalt fibers limit crack initiation and propagation, thereby contributing to improved tensile resistance [68].

By contrast, the water-to-cement ratio does not exhibit a significant independent effect within the investigated range. The GP×BF interaction term, although statistically significant, indicates a limited interaction effect, pointing to a delicate balance between matrix refinement provided by GP and the efficiency of fiber reinforcement. Similar trends have been reported in the literature, where excessive fiber contents or combined additions can reduce effectiveness due to workability and dispersion limitations [74]. Overall, these findings confirm that tensile strength improvement is mainly governed by the combined use of GP and BF, provided that their proportions are carefully optimized.

The diagnostic plots reveal a strong correspondence between the observed and predicted tensile strength values, demonstrating that the regression model effectively represents the tensile response of concrete mixtures incorporating glass powder (GP) and basalt fiber (BF) (Fig. 8.6). This correspondence highlights the role of finely ground glass powder in improving particle packing and strengthening the paste–aggregate interface, thereby mitigating microstructural defects and contributing to enhanced tensile performance [53, 69]. The absence of systematic deviation further indicates that the influence of GP has been consistently captured within the examined replacement levels.

In addition, the standardized residuals are randomly scattered around zero, with no evident trends or variance amplification, confirming the adequacy of the linearity and homoscedasticity assumptions, even when the GP×BF interaction term is included. This behavior suggests that the contribution of basalt fibers in restraining crack initiation and propagation—through effective crack-bridging

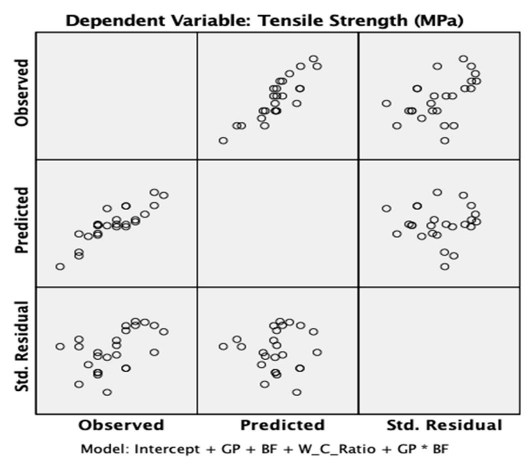

Figure 8.6. Diagnostic plot of model assumptions for tensile strength.

Table 8.6.1. Tests of between-subjects effects of GP, BF, W/C ratio on tensile strength.

Source	Type III Sum of Squares	df	Mean Square	F	Sig.	Partial Eta Squared
Corrected Model	1.433[a]	4	0.358	15.404	0.000	0.755
Intercept	0.292	1	0.292	12.544	0.002	0.385
GP	1.159	1	1.159	49.844	0.000	0.714
BF	0.388	1	0.388	16.704	0.001	0.455
W/C Ratio	0.043	1	0.043	1.834	0.191	0.084
GP * BF	0.520	1	0.520	22.372	0.000	0.528

R Squared = 0.755 (Adjusted R Squared = 0.706).

Table 8.6.2. Regression coefficients of GP, BF, W/C and GP*BF on tensile strength.

					95% Confidence Interval	
Parameter	B	Std. Error	t	Sig.	Lower Bound	Upper Bound
Intercept	4.400	1.242	3.542	0.002	1.808	6.991
GP	0.014	0.002	7.060	0.000	0.010	0.018
BF	0.057	0.014	4.087	0.001	0.028	0.086
W/C Ratio	–4.074	3.009	–1.354	0.191	–10.350	2.202
GP * BF	–0.001	0.000	–4.730	0.000	–0.002	–0.001

and stress redistribution mechanisms—has been appropriately reflected in the model [72]. As a result, the proposed model can be regarded as statistically robust for both interpretation and prediction of tensile strength in GP–BF concrete mixtures within the investigated parameter domain.

8.7. Assessment of flexural strength

The multivariable statistical modeling approach results show that the proposed model accounts for a substantial share of the variation in flexural strength ($R^2 = 0.807$), with glass powder (GP) emerging as the main statistically significant contributor (Tables 8.7.1 and 8.7.2). This finding is consistent with earlier studies demonstrating that finely ground glass powder improves flexural performance by enhancing matrix continuity and promoting more efficient load transfer under bending conditions [19, 72].

Although basalt fiber (BF) and the water-to-cement ratio do not exhibit significant independent effects within the investigated range, the GP×BF interaction is statistically significant, pointing to a sensitive interplay between matrix refinement and fiber efficiency. Similar trends have been reported in the literature, where the combined use of mineral admixtures and fibers leads to improved flexural behavior when mixture proportions are carefully optimized to minimize dispersion issues and workability constraints [61]. Overall, these results indicate that flexural strength improvement is primarily driven by GP incorporation, with the combined GP–BF system providing a supportive yet proportion-dependent contribution.

The diagnostic plots indicate a close alignment between observed and predicted flexural strength values, confirming that the regression model satisfactorily represents the flexural behavior of concrete mixtures containing GP and BF (Fig. 8.7). This alignment reflects the positive contribution of GP to improving matrix continuity and stress transfer under bending loads, which enhances flexural performance [53].

Furthermore, the absence of heteroscedastic patterns in the standardized residuals supports the validity of the model assumptions. This behavior suggests that the contribution of basalt fibers to flexural strength through energy absorption and delayed crack propagation has been appropriately captured, ensuring the robustness of flexural strength predictions [78].

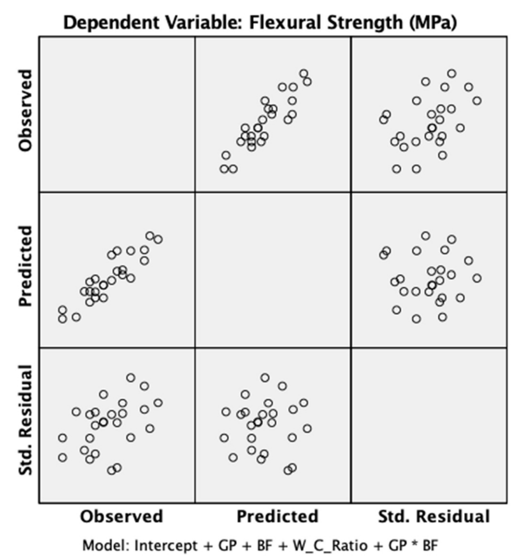

Figure 8.7. Diagnostic plot of model assumptions for flexural strength.

Table 8.7.1. Tests of between-subjects effects of GP, BF, W/C ratio on flexural strength.

Source	Type III Sum of Squares	df	Mean Square	F	Sig.	Partial Eta Squared
Corrected Model	17.122[a]	4	4.280	20.923	0.000	0.807
Intercept	2.758	1	2.758	13.480	0.002	0.403
GP	9.483	1	9.483	46.355	0.000	0.699
BF	0.558	1	0.558	2.729	0.114	0.120
W/C Ratio	0.443	1	0.443	2.166	0.157	0.098
GP * BF	1.779	1	1.779	8.698	0.008	0.303

a. R Squared = 0.807 (Adjusted R Squared = 0.769).

Table 8.7.2. Regression coefficients of GP, BF, W/C and GP*BF on flexural strength.

Parameter	B	Std. Error	t	Sig.	95% Confidence Interval Lower Bound	95% Confidence Interval Upper Bound
Intercept	13.529	3.685	3.672	0.002	5.843	21.215
GP	0.040	0.006	6.808	0.000	0.028	0.053
BF	0.068	0.041	1.652	0.114	–0.018	0.154
W/C Ratio	–13.135	8.925	–1.472	0.157	–31.752	5.482
GP * BF	–0.002	0.001	–2.949	0.008	–0.004	–0.001

8.8. Interactive influence of BF and GP on concrete properties

For the combined impact of BF and GP, we developed contour plots. The contour plot illustrates in Fig. 8.8.1 the interactive influence of BF and GP content on the freeze-thaw resistance of high-performance concrete. As seen in the plot, freeze-thaw resistance generally increases with both BF and GP content. The highest resistance values, exceeding 93%, are observed when BF is around 0.4% and GP reaches 20%, showing the synergistic effect at these levels. Moderate combinations, such as 0.2% BF with 5–15% GP, also yield improved resistance compared to the lower end of the spectrum. On the other hand, low BF and GP levels correspond to the lowest freeze-thaw resistance, indicating that the inclusion of these materials plays an important role in enhancing durability under cyclic freezing and thawing conditions. The smooth gradient in the plot shows an upward trend in strength as the dosage of both BF and GP increases.

The contour plot illustrates in Fig. 8.8.2 the variation in 28-day compressive strength (in MPa) of a

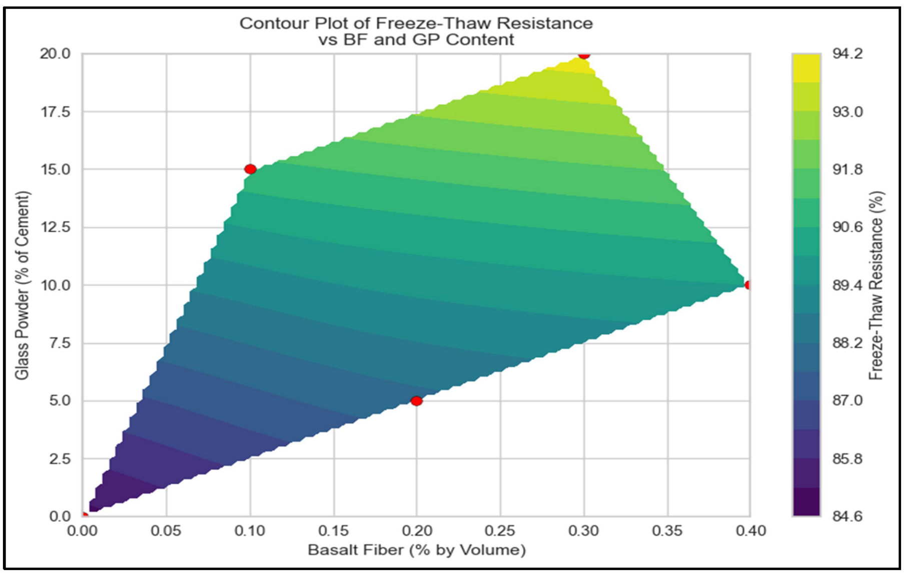

Figure 8.8.1. Contour plot of freeze - thaw resistance vs BF and GP content.

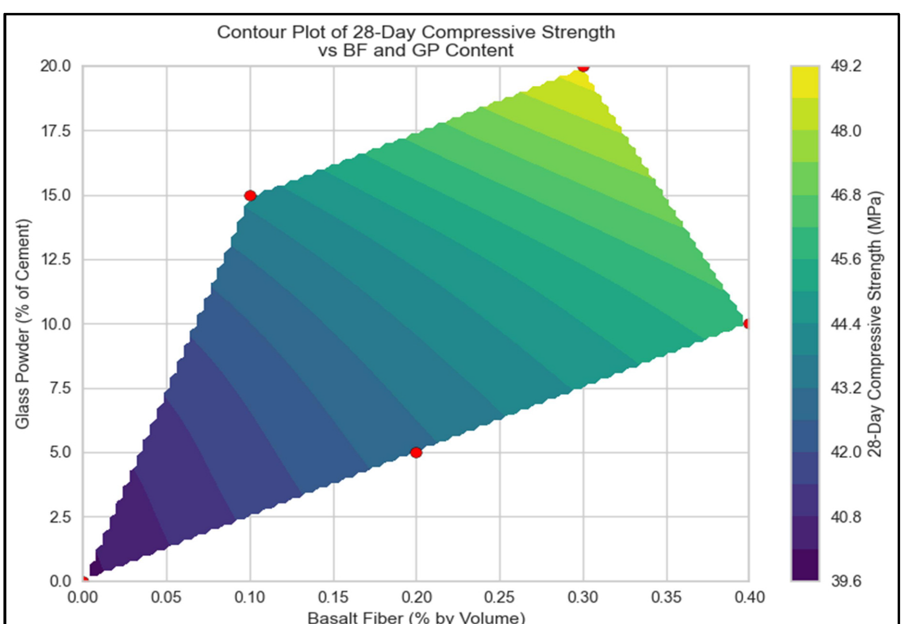

Figure 8.8.2. Contour plot of 28-day compressive strength vs BF and GP content.

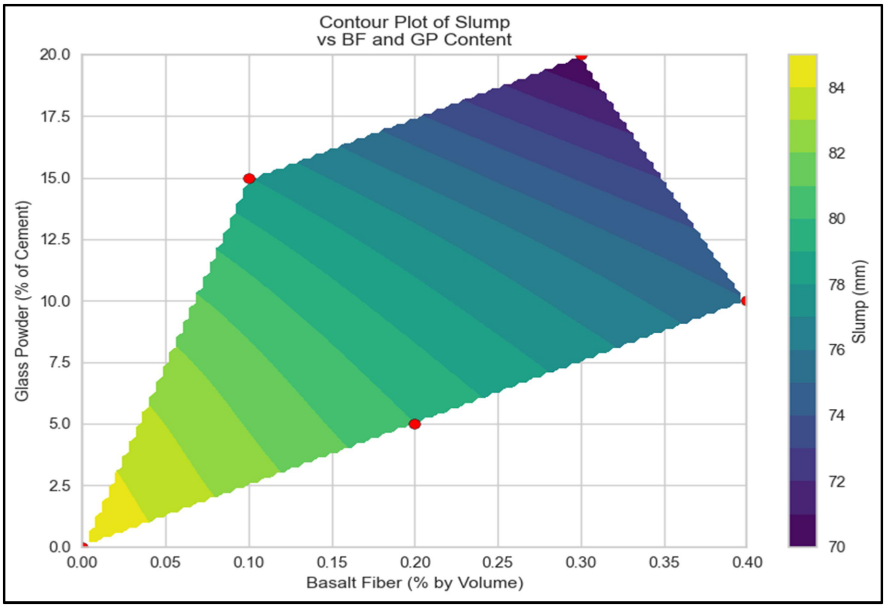

Figure 8.8.3. Contour plot of slump vs BF and GP content.

cementitious mixture as a function of BF content (% by volume) and GP content (% of cement). The plot reveals a clear trend: as both BF and GP content increase, the compressive strength also improves. This trend is represented by the gradient of color from dark purple (indicating lower strength around 39.6 MPa) to bright yellow (indicating higher strength, peaking at approximately 49.2 MPa). The highest compressive strength is observed in the region where BF is around 0.4% and GP is close to 20%, showing the synergistic effect of these additives at higher concentrations. Conversely, the lowest strength occurs when both BF and GP are near zero. The red dots on the plot mark specific experimental data points used in the interpolation, providing a reference for the model's basis.

Similarly, the contour plot in Fig. 8.8.3 shows the variation in slump of a concrete mix in relation to the content of BF and GP. From the plot, it is evident that slump decreases with increasing BF and GP content. The highest slump values (around 85 mm, shown in yellow) occur when both BF and GP contents are near zero, indicating that the mix is most workable without these additives. As BF increases to 0.4% and GP rises to 20%, the slump drops significantly to about 70 mm (dark purple region), showing reduced workability. This reduction is likely due to the stiffening effect of BFs and the finer particle nature of GP, both of which can absorb water and reduce fluidity.

The plot in Fig. 8.8.4 indicates that flexural strength improves with increasing percentages of both BF and GP. The highest values (~11 MPa) are observed when BF is at 0.3–0.4% and GP is at 20%. This shows a synergistic enhancement in flexural performance when both additives are optimally combined. A similar trend is observed for tensile strength (Fig. 8.8.5), where both additives contribute positively. The strength increases from ~2.8 MPa (with no additives) to ~3.8 MPa with 0.4% BF and 20% GP. This reinforces the beneficial role of BF and GP in improving the tensile properties of the mix.

9. Discussion

The trends observed in workability, mechanical properties, and durability are interpreted primarily on the basis of macroscopic test results, supported by well-established findings reported in the literature. Although direct microstructural characterization techniques, such as SEM, XRD, or MIP, were not employed in this study, the improvements associated with increasing glass powder (GP) content can be discussed in light of previously reported mechanisms. These mechanisms commonly include filler effects, improved particle packing, and the pozzolanic activity of finely ground glass, all of which have been shown to contribute to matrix densification and enhanced interfacial bonding.

The consistent enhancement in strength and durability-related properties with GP incorporation may therefore be viewed as an indirect indication of a refined cementitious matrix, as reflected by the measured performance indicators. Likewise, the observed improvement in workability is likely related to the fineness and smooth surface characteristics of GP

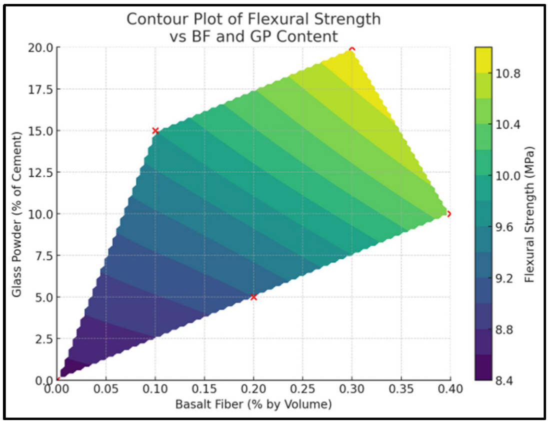

Figure 8.8.4. Contour plot of flexural strength vs BF and GP content.

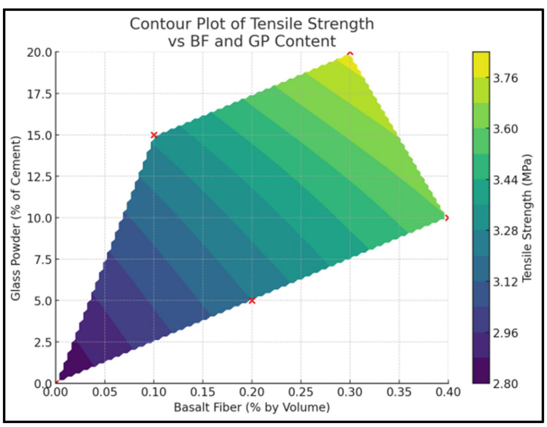

Figure 8.8.5. Contour plot of tensile strength vs BF and GP content.

particles, which influence paste rheology rather than direct fiber–matrix interaction. These explanations are presented as plausible interpretations rather than direct microstructural evidence and are supported by relevant studies in the existing literature.

Accordingly, the discussion has been structured to clearly differentiate between experimentally observed outcomes and mechanism-based interpretations drawn from prior research. Further studies incorporating direct microstructural characterization are recommended to validate these interpretations and to provide a more detailed understanding of the underlying mechanisms.

9.1. Interpretation of results

Some interpretations of the predicted results based on the obtained results can be presented here. It can be concluded that both hypotheses in this work revealed a good relationship and a direct interaction between the constituents. This interaction increased both performances because of the internal packing effects. The basalt fiber has a chemical composition similar to that of basalt rocks, which can produce a chemical bond to the HPBFC ingredients. The glass powder is a silica-alumina-silica material, which crystallizes between CSH whiskers to strengthen the bonding between the constituents. Thus, the formulated hypotheses are true, and the results clearly state that HPBFC can be produced with high strengths. The level and increments of the concrete strengths depend on the quantity of the glass powder. The change of the microstructure in HPBFC can significantly determine the change in strength. The better the characteristics of the microstructure of the HPBFCs, the higher the strength of the HPBFCs. When the microstructure is changed from a dense to a less porous phase, and the VRR of AFm is increased, the content of the AFm is estimated to be prolonged. Thus, the growth of the strength and morphological changes of viscous material, such as cementitious bonding paste, can be seen to be also acceptable. The predictions have also been made very precisely regarding merging HPBFC characteristics from the ESEM, XRD, and mechanical strength obtained, according to the results obtained in this research work. The material specifications of the cementitious components of vitrified, which are h-wollastonite, the new crystalline phases of the contact, and probably nepheline, were very visible in the XRD diagrams of the HPBFC3 and HPBFC2 mixes. The values increased after 28 curing days, thus improving the morphological characteristics of the mix. These findings are incapable of describing the high values of the obtained quantity of silicon and the alkalis, which are ascertained by the decrease in the value of mass loss in the above-mentioned mix. This increased with a few exposures to load and was noted in the presentation of less than the variation of the oil content of the mix, making the loss less than 1.25%. Finally, we can conclude that the results of this study are exactly well predicted according to the base assumptions of the work.

9.2. Comparison with existing studies

This study evaluates only high-performance basalt fiber concrete (HPBFC), which is generally stronger and more workable than conventional BFC. The obtained findings were compared with those of BFC. The consistency of the outcomes with those of BFC strengthens the potential for utilizing glass powder as a sustainable material in HPBFC. A comparison of the obtained outcomes with the existing results is summarized. There are many studies concerning the effect of various materials on BFC, meaning a variety of data are available regarding normal BFC with historical methods. However, the available data could already serve as a representative benchmark for assessing the effects of glass powder on concrete. This study evaluated the effect of 5–25% glass powder contents on high performance basalt fiber concrete (HPBFC). Experimental testing showed that optimum 5% fly ash replacement with 15% glass powder exhibited the highest compressive and flexural strengths. Other higher glass contents led to continuous strength reductions. This shows that the use of geopolymer led to the need for special curing, and that the curing temperature affected the concrete properties. Testing 0–40% glass powder content on the replacement of cement performance indicated that 10% glass content showed the maximum value and 15% glass content showed strength loss. Common points obtained from the performances on new sustainable materials studies covering high performance fiber reinforced concrete can be shown as follows: researchers believe that the use of eco-friendly energy and raw materials in concrete is vital for raising sustainable development. As concrete sustainability increases, there is an increasing need for using sustainable materials integrated into concrete. Additionally, there are some points that need more research to fill the existing gaps. The effectiveness of blending time, space, climate, and the proportion of this kind of concrete placed at the construction site can be questioned.

10. Conclusion and future directions

This study evaluated the influence of GP as a partial cement replacement and BF as a reinforcing agent on the mechanical, durability, and slump properties of high-performance concrete. A comprehensive statistical analysis, including multivariable statistical modeling approach and Tukey's HSD post-hoc tests, was carried out to assess the effects of varying GP (0–20%) and BF (0–0.6%) contents on freeze-thaw resistance, compressive strength, flexural strength, tensile strength, and slump. The interactive influence of GP and BF was then visualized using the contour plots. The result indicate that the GP plays an important role in increasing both strength and durability. A 20% GP replacement resulted in the greatest improvement in compressive strength, with an increase of approximately 16.33 MPa at 180 days compared to the control mix (0% GP). The Flexural and tensile strengths also improved significantly at GP contents of 10% and above. The freeze-thaw resistance improved as the amount of GP increased, with the mix containing 20% GP, which shows the greatest durability when exposed to repeated cycles of freezing and thawing. The BF content did not result in any statistically significant improvements in the compressive, tensile, or flexural strengths across all curing ages. Slump was significantly reduced with increasing BF content, this reduction becomes more pronounced at fiber contents exceeding 0.3% by volume and is likely associated with the increased surface area and interlocking characteristics of the fibers, which restrict flow and increase internal friction within the fresh mixture. While the incorporation of glass powder (GP) has demonstrated clear improvements in strength and durability, and basalt fibers (BF) primarily influence workability, further investigation is required to optimize their combined use in high-performance concrete.In addition, future studies incorporating life-cycle assessment (LCA) and cost–benefit analysis would provide a more comprehensive evaluation of the practical feasibility and sustainability benefits associated with the use of GP and BF in construction applications.

10.1. Summary of findings

This paper presents the results of empirical research into the use of high-performance basalt fiber concrete (HPBFC) with glass powder from waste glass. The research involved an experimental evaluation of the efficiency of HPBFC with waste glass, namely glass powder, in terms of its mechanical properties, such as compressive strength, tensile strength, and flexural strength, in terms of the workability of fresh concrete, and in the context of the material's durability. Such tests, both on the fresh state and hardened state, are supported by microstructural results to reveal the microstructures and elemental compositions.

In general, the obtained experimental results showed that the glass powder had a promising effect on the performance of high-performance basalt fiber concrete. This is because, in each test, namely concrete strength (compressive, split tensile, and flexural strengths), axial strain capacity, elasticity modulus, and workability, the test results were similar for the three concrete strengths with glass powder at 7.5%, 10%, and the control, and were higher than that of the reference concrete at 5%. Furthermore, the shear retention capacity and modulus of elasticity retention were in line with the tensile strength. These include the fact that the three concrete strengths tested with glass powder could last longer in certain environmental conditions due to the increased durability and reduction in porosity obtained in the microstructural investigation.

It was also found that glass powder has the potential to lower the strength when added to concrete. In the aspect of workability, due to the requirement to use more superplasticizer to improve workability based on the slump, glass powder has a promising effect due to its potential efficiency (the water demand is reduced). This point is very important concerning the use of crushed basalt and BFRP in concrete as advanced concrete with sustainable issues and to make it environmentally friendly and safe for modern building construction. The main challenges encountered in this study were the poor adhesion of the HPBFC-glass powder and the significant slump drop, both as a result of the increasing amount of glass powder.

10.2. Implications for practice and research

In practice, the findings indicate that glass powder usage in high-performance basalt fiber concrete has few issues with strength, workability, durability, and microstructure performance, and thus can be applied confidently for both sustainability and, to some degree, performance concerns in the construction industry. In addition, it can be expected that concrete sustainability will become an industry standard and be included in industrial quality management standards as sustainability reputation is increasingly related to consumer choices through increasing environmentally friendly mechanisms. Therefore, as new research is increasingly being investigated for the production of environmentally friendly, energy-efficient, and sustainable materials in interdisciplinary areas, it is likely that today's deserts will move towards preserving these new research reforms and high quality in the future. Highlighting applications will provide insights into the motivations for such research and the standards applicable to the construction industry and related fields in order to meet tomorrow's needs.

Research into the circulation and performance of glass powder as a modern concrete addition can be considered a requirement for sustainable raw materials development. It is thus proposed that further studies be conducted for engineers, practitioners, and scholars. For future studies, it is important for researchers interested in interdisciplinary research areas to conduct parallel studies to investigate the microstructure of glass powder in innovative organic combinations with these materials, nano-based, or mixed. Furthermore, the combined work of the material mechanics and chemical science fields on sustainability and concrete applications will provide insight into future creation. From the various applications, it is an engineering and research practice to preserve the quality and modernity of today's materials. In order to address the scarcity of resources in the world and the higher quality requirements of today, we must work hard to find new research pathways and to work on high-performance and long-lasting materials. Research may continue to open such new doors from interrelated areas, as discussed here today, in order to foster greater advances in the field.

Acknowledgments

The author is thankful to the Deanship of Graduate Studies and Scientific Research at University of Bisha for supporting this work through the Fast-Track Research Support Program.

Conflict of interest

The author declare no conflict of interest.

Data availability

The author confirms that the data supporting the findings of this study are available within the article.

References

1. Nassar AK, Palanimurugan R, Kathirvel P, Murali G, Dixit S. Innovative approaches to sustainable powder activator production from silica-rich industrial waste for clinker-free one-part binders in Green Construction Materials. *Innovative Infrastructure Solutions*. 2025;10(12). https://doi.org/10.1007/s41062-025-02306-1.
2. Nassar AK, Sivanandam S, Saran D, Siyaam Sundar SB, Kathirvel P, Murali G, Dixit S. Durability assessment of sustainable one-part alkali activated concrete produced from agricultural and industrial waste activators under aggressive environmental conditions. *Construction and Building Materials*. 2025; 486: 141823. https://doi.org/10.1016/j.conbuildmat.2025.141823.
3. Nassar AK, Kathirvel P, Murali G. Fracture behavior of sustainable activators-based fibrous alkali-activated concrete under mode I, I/III & III loading. *Structural Engineering and Mechanics*. 2025;93(4):247–267. https://doi.org/10.12989/SEM.2025.93.4.247.
4. Murali G, Nassar AK, Swaminathan M, Kathirvel P, Wong LS. Effect of silica fume and glass powder for enhanced impact resistance in GGBFS-based ultra high-performance geopolymer fibrous concrete: An experimental and statistical analysis. *Defence Technology*. 2024;41:59–81. https://doi.org/10.1016/j.dt.2024.05.015.
5. Salahaddin SD, Haido JH, Wardeh G. Rheological and mechanical characteristics of basalt fiber UHPC incorporating waste glass powder in lieu of cement. *Ain Shams Engineering Journal*. 2023. https://doi.org/10.1016/j.asej.2023.102515.
6. Selvakumar M, Geetha S, Rangan SK, Sithrubi T, Sathyashriya K. Effect of glass powder as partial fine aggregate replacement on properties of basalt fibre reinforced concrete. *Materials Today: Proceedings*. 2020. https://doi.org/10.1016/j.matpr.2020.09.299.
7. Mohammadyan-Yasouj SE, Ghaderi A. Experimental investigation of waste glass powder, basalt fibre, and carbon nanotube on the mechanical properties of concrete. *Construction and Building Materials*. 2020; 252: 119115. https://doi.org/10.1016/j.conbuildmat.2020.119115.

8. Wang D, Han L, Ju Y, Bai J, Fan Y. Experimental study on tensile properties of basalt fiber reactive powder concrete. *Strength of Materials.* 2021;53(4):670–674. https://doi.org/10.1007/s11223-021-00330-x.
9. Kočí V, Vejmelková E, Koňáková D, Pommer V, *et al.* Basic properties of reactive powder concrete with basalt and polypropylene fibers after high-temperature exposure. *Construction and Building Materials.* 2023:130922. https://doi.org/10.1016/j.conbuildmat.2023.130922.
10. Khan MNN, Jamil M, Karim MR, Zain MFM. Sustainable utilization of recycled glass powder in high-performance concrete: Microstructure and lifecycle assessment. *Journal of Cleaner Production.* 2022;330:129851. https://doi.org/10.1016/j.jclepro.2021.129851.
11. Shi C, Zheng K. A review on the use of waste glasses in the production of cement and concrete. *Resources, Conservation and Recycling*. 2007;52(2):234–247. https://doi.org/10.1016/j.resconrec.2007.01.013.
12. Abbas S, Nehdi ML, Saleem MA. Synergistic effects of basalt fiber and glass powder in eco-efficient concrete: Mechanical performance and interfacial bonding. *Materials Today Communications*. 2023;34:105231. https://doi.org/10.1016/j.mtcomm.2022.105231.
13. Zhang L, Wang H, Li X. Machine learning-driven optimization of fiber-reinforced concrete: A comparative study of ensemble models. *Cement and Concrete Composites*. 2021;123:104198. https://doi.org/10.1016/j.cemconcomp.2021.104198.
14. Aydın S, Baradan B. Performance of hybrid basalt fiber-geopolymer composites under thermal and mechanical stress. *Composite Structures.* 2022;284:115182. https://doi.org/10.1016/j.compstruct.2021.115182.
15. Gupta T, Sharma RK, Chaudhary S. Recycled glass-basalt epoxy composites for sustainable infrastructure repair: Abrasion and adhesion performance. *Journal of Materials in Civil Engineering*. 2023;35(4):04023012. https://doi.org/10.1061/(ASCE)MT.1943-5533.0004567.
16. Wang Y, Liu X, Zhang Q. Dynamic modulus enhancement and damping behavior of basalt fiber-reinforced concrete under cyclic loading. *Engineering Structures*. 2022;256:114023. https://doi.org/10.1016/j.engstruct.2022.114023.
17. Li H, Zhang Y, Wang J. Durability of basalt fibers in alkaline environments: Degradation mechanisms and predictive models. *Materials and Structures.* 2021;54(2):78. https://doi.org/10.1617/s11527-021-01663-4.
18. Patel R, Kumar S. Scalability challenges in low-carbon ultra-high-performance concrete: A roadmap for industrial adoption. *Sustainable Materials and Technologies*. 2023;35:e00528. https://doi.org/10.1016/j.susmat.2022.e00528.
19. Shi C, Wu Y, Riefler C, Wang H. Characteristics and pozzolanic reactivity of glass powders. *Cement and Concrete Research*. 2005;35(5):987–993.
20. Matos AM, Sousa-Coutinho J. Durability of mortar using waste glass powder as cement replacement. *Construction and Building Materials*. 2012;36:205–215.
21. Taha B, Nounu G. Properties of concrete contains mixed colour waste recycled glass as sand and cement replacement. *Construction and Building Materials*. 2008;22(5):71720.
22. Militký J, Mishra R, Lenfeldová I. Mechanical behavior of basalt and glass fiber-reinforced concrete. *Procedia Engineering*. 2014;95:525–531.
23. Belkadi M, Chaid R, Perrot A. Valorization of glass powder waste, crushed and dune sands in the mix design of ultra-high performance fiber reinforced concrete: Assessing effect of waste variability. *Matériaux & Techniques*. 2021;109:103. https://doi.org/10.1051/MATTECH/2021015.
24. Khudair AY, Mohammed M, Hama SM. Optimization of glass powder content in self-compacting concrete as partial replacement of cement. *IOP Conference Series: Materials Science and Engineering*. 2020;928(2). https://doi.org/10.1088/1757-899X/928/2/022140.
25. Shoaib S, El-Maaddawy T, El-Hassan H, El-Ariss B, Alsalami M. Fresh and hardened properties of concrete reinforced with basalt macro-fibers. *Buildings*. 2022;12(8):1136. https://doi.org/10.3390/buildings12081136.
26. Elshazli MT, Ramirez K, Ibrahim A, Badran M. Mechanical, durability and corrosion properties of basalt fiber concrete. *Fibers*. 2022;10(2):10. https://doi.org/10.3390/fib10020010.
27. Tariq S, Scott A, Mackechnie J, Shah V. Glass powder replacement in self-compacting concrete and its effect on rheological and mechanical properties. *Journal of Sustainable Cement-Based Materials*. 2021;11(3):240–256. https://doi.org/10.1080/21650373.2021.1922948.
28. Çelik Z, Bingöl AF. Fracture properties and impact resistance of self-compacting fiber reinforced concrete (SCFRC). *Materials and Structures*. 2020;53(1):1–16. https://doi.org/10.1617/s11527-020-01487-8.
29. Ruben N, Venkatesh C, Durga C, Chand M. Comprehensive study on performance of glass fibers-based concrete. *Innovative Infrastructure Solutions*. 2021;6(1):1–11. https://doi.org/10.1007/s41062-021-00490-4.
30. Moceikis R, Karpova E, Kičaitė A, Skripkiūnas G. Effect of aggregates on the technological and mechanical properties of glass and basalt fibres reinforced concrete. *IOP Conference Series: Materials Science and Engineering*. 2019;471(3). https://doi.org/10.1088/1757-899X/471/3/032008.
31. Olukayode OM, Akinwande AA, Balogun OA, Oyediran AO, Mosuru SG. Applicability of the response surface method in the optimization of compressive strengths of banana-fiber-reinforced concrete using waste glass as partial cement replacement. *Innovative Infrastructure Solutions*. 2023;8(8):207. https://doi.org/10.1007/s41062-023-01178-7.
32. Xu L, Song D, Liu N, Liu W. Study on mechanical properties of basalt fiber-reinforced concrete with high content of stone powder at high temperatures. *Advances in Materials Science and Engineering*. 2021;2021:7517049. https://doi.org/10.1155/2021/7517049.
33. Borhan TM. Properties of glass concrete reinforced with short basalt fibre. *Materials & Design*. 2012;42:265–271. https://doi.org/10.1016/j.matdes.2012.05.062.
34. Wang D *et al.* Mechanical properties of ultra-high performance fiber reinforced concrete. *Construction and Building Materials*. 2019;234:117390. https://doi.org/10.1016/j.conbuildmat.2019.117390.
35. Kizilkanat AB *et al.* Mechanical properties and fracture behavior of high-strength concrete reinforced with basalt and glass fibers. *Construction and Building Materials*. 2015;100:218–224. https://doi.org/10.1016/j.conbuildmat.2015.10.006.
36. Kavya BR *et al.* Prediction of strength properties of basalt fiber reinforced concrete using artificial neural networks. *Asian Journal of Civil Engineering*. 2022;23:877–886. https://doi.org/10.1007/s42107-022-00460-w.
37. Zhao H, Wang L, Wang D, Bai J, Fan Y. Effect of basalt fiber on chloride ion penetration of reactive powder concrete. *IOP Conference Series: Materials Science and Engineering*. 2020;711:012067. https://doi.org/10.1088/1757-899X/711/1/012067.
38. Graybeal B, Tanesi J. Durability of an ultra-high-performance concrete. *Journal of Materials in Civil Engineering*. 2007;19(10):848–854. https://doi.org/10.1061/(ASCE)0899-1561(2007)19:10(848).

39. Li W, Liu H, Zhu B, Lyu X, Gao X, Liang C. Mechanical properties and freeze–thaw durability of basalt fiber reactive powder concrete. *Applied Sciences*. 2020;10(16):5682. https://doi.org/10.3390/app10165682.
40. Cai Z, Ren J, Shen G, Jin C, Gu X, Cheng W, Wang H. Influence of assembly unit of fibers on the mechanical and long-term properties of reactive powder concrete. *Coatings*. 2023;13(2):412. https://doi.org/10.3390/coatings13020412.
41. Kim IS, Choi SY, Yang E. Evaluation of durability of concrete substituted heavyweight waste glass as fine aggregate. *Construction and Building Materials*. 2018. https://doi.org/10.1016/J.CONBUILDMAT.2018.06.221.
42. Qi Z, Liu Y, Zhang W. Study on salt-frost damage durability of high-performance concrete with polypropylene fiber. *Materials*. 2025. https://doi.org/10.3390/ma18051007.
43. Grzeszczyk S, Matuszek-Chmurowska A, Vejmelková E, Černý R. Reactive Powder Concrete Containing Basalt Fibers: Strength, Abrasion and Porosity. *Materials*. 2020;13. https://doi.org/10.3390/ma13132948.
44. Xu J, Kang A, Wu Z, Xiao P, Gong Y. Evaluation of workability, microstructure and mechanical properties of recycled powder geopolymer reinforced by waste hydrophilic basalt fiber. *Journal of Cleaner Production*. 2023. https://doi.org/10.1016/j.jclepro.2023.136514.
45. Cui S, Liu P, Cui E, Su J, Huang B. Experimental study on mechanical property and pore structure of concrete for shotcrete use in hot-dry tunnel environments. *Construction and Building Materials*. 2018. https://doi.org/10.1016/J.CONBUILDMAT.2018.03.191.
46. Liu F, Ding W, Qiao Y. An experimental investigation on the integral waterproofing capacity of polypropylene fiber concrete. *Construction and Building Materials*. 2019. https://doi.org/10.1016/J.CONBUILDMAT.2019.04.027.
47. Yu Q, Chen Z, Yang L, Mukhopadhyaya P, Zhang L, Wu Q, Ni L, Mi Q. Preparation and characterisation of glass fibre–fumed silica composite core material VIP. *Physics and Chemistry of Glasses*. 2022. https://doi.org/10.13036/17533562.63.3.21.
48. PehlivanlıZO, Uzun I, Demir I. Mechanical and microstructural features of autoclaved aerated concrete reinforced with fibers. *Construction and Building Materials*. 2015;96:428–433. https://doi.org/10.1016/J.CONBUILDMAT.2015.08.104.
49. Wu H, Zhao J, Wang Z. Study on Micro-Structure and Durability of Fiber Concrete. *Research Journal of Applied Sciences, Engineering and Technology*. 2013;5:659–664. https://doi.org/10.19026/RJASET.5.5005.
50. Kim E, Kim K, Song O. Properties of basalt-fiber reinforced foam glass. *Journal of Asian Ceramic Societies*. 2020;8:170–175. https://doi.org/10.1080/21870764.2020.1718858.
51. Liu J, Shuo Z, Runqing L. Study on antifreeze Properties and pore structure of Basalt Fiber Reinforced Concrete. *Journal of Physics: Conference Series*. 2020;1605. https://doi.org/10.1088/1742-6596/1605/1/012151.
52. Du H, Tan K. Properties of high-volume glass powder concrete. *Cement & Concrete Composites*. 2017;75:22–29. https://doi.org/10.1016/J.CEMCONCOMP.2016.10.010.
53. Shao Y, Lefort T, Moras S, Rodriguez D. Studies on concrete containing ground waste glass. *Cement and Concrete Research*. 2000;30(1):91–100. https://doi.org/10.1016/S0008-8846(99)00213-6.
54. Taha B, Nounu G. Utilizing waste recycled glass as sand/cement replacement in concrete. *Journal of Materials in Civil Engineering*. 2009;21(12):709–721. https://doi.org/10.1061/(ASCE)0899-1561(2009)21:12(709).
55. Du H, Tan KH. Effect of particle size on alkali–silica reaction mitigation using glass powder. *Cement and Concrete Composites*. 2014;45:223–233. https://doi.org/10.1016/j.cemconcomp.2013.10.011.
56. Shayan A, Xu A. Performance of glass powder as a pozzolanic material in concrete: A field trial on concrete slabs. Cement and Concrete Research. 2006; 36(3): 457–468. https://doi.org/10.1016/j.cemconres.2005.10.008.
57. Nassar RUD, Soroushian P. Field application of concrete incorporating milled waste glass. *Journal of Materials in Civil Engineering*. 2012;24(10):1323–1330. https://doi.org/10.1061/(ASCE)MT.1943-5533.0000489.
58. Rajabipour F, Maraghechi H, Fischer G. Investigating the alkali-silica reaction of recycled glass aggregates in concrete materials. *Journal of Materials in Civil Engineering*. 2010;22(12):1201–1208. https://doi.org/10.1061/(ASCE)MT.1943-5533.0000136.
59. Corinaldesi V, Gnappi G, Moriconi G, Montenero A. Reuse of ground waste glass as aggregate for mortars. *Waste Management*. 2005;25(2):197–201. https://doi.org/10.1016/j.wasman.2004.07.010.
60. Fiore V, Di Bella G, Valenza A. The effect of basalt fibre on mechanical properties of a cement based mortar. *Construction and Building Materials*. 2011;25(2):891–896. https://doi.org/10.1016/j.conbuildmat.2010.06.063.
61. Sim J, Park C, Moon DY. Characteristics of basalt fiber as a strengthening material for concrete structures. *Composites Part B: Engineering*. 2005;36(6–7):504–512. https://doi.org/10.1016/j.compositesb.2005.02.002.
62. Branston J, Das S, Kenno SY, Taylor C. Mechanical behaviour of basalt fibre reinforced concrete. *Construction and Building Materials*. 2016;124:878–886. https://doi.org/10.1016/j.conbuildmat.2016.08.009.
63. Ayub T, Shafiq N, Nuruddin MF. Mechanical properties of high-performance concrete reinforced with basalt fibers. *Construction and Building Materials*. 2014;50:347–358. https://doi.org/10.1016/j.proeng.2014.07.016.
64. Savi P, Corinaldesi V. Sustainable fiber-reinforced concretes with basalt fibers and recycled aggregates. *Construction and Building Materials*. 2020;238:117583. https://doi.org/10.1016/j.conbuildmat.2019.117583.
65. Bheel N, Khahro SH, Shaikh MA, Memon SA, Solangi MM. Synergistic effect of basalt fibers and glass powder on the strength and durability of concrete. *Case Studies in Construction Materials*. 2022;16:e01028. https://doi.org/10.1016/j.cscm.2022.e01028.
66. Du H, Tan KH. Properties of high volume glass powder concrete. *Cem Concr Compos.* 2017;75:22–29. doi:10.1016/j.cemconcomp.2016.10.010.
67. Jiang C, Fan K, Wu F, Chen D. Experimental study on the mechanical properties and microstructure of chopped basalt fibre reinforced concrete. *Mater Des.* 2014;58:187–193. 10.1016/j.matdes.2014.01.056.
68. Afshinnia K, Rangaraju PR. Impact of combined use of ground glass powder and crushed glass aggregate on selected properties of Portland cement concrete. *Constr Build Mater*. 2016;117:263–272. doi:10.1016/j.conbuildmat.2016.04.072.
69. Al-Kharabsheh BN, Arbili MM, Majdi A, *et al.* Basalt Fibers Reinforced Concrete: Strength and Failure Modes. *Materials (Basel)*. 2022;15(20):7350. doi:10.3390/ma15207350.
70. Nassar RUD. Heat of hydration, water sorption and microstructural effects of waste glass powder in cementitious systems. *Cogent Eng.* 2024;11(1):2297466. doi:10.1080/23311916.2023.2297466.

71. Wu H, Qin X, Huang X, Kaewunruen S. Engineering, mechanical and dynamic properties of basalt fiber reinforced concrete. *Materials (Basel)*. 2023;16(2):623. doi:10.3390/ma16020623.
72. Wang Z, Fu C, Wang K, Zhao J, Shumuye ED, Yang Z. Effect of geopolymer concrete cover on improving tensile and transverse shear behaviors of BFRP bars after exposure to high temperature. *Case Stud Constr Mater*. 2024;20:e02862. doi:10.1016/j.cscm.2024.e02862.
73. Alnahhal W, Alengaram UJ, Jumaat MZ. Mechanical, durability and microstructural properties of basalt fiber reinforced concrete: A comprehensive review. *Fibers*. 2022;10(2):10.doi:10.3390/fib10020010.
74. Banthia, Nemkumar, and Jean-François Trottier. Concrete reinforced with deformed steel fibers, Part II: Toughness characterization. *ACI Materials Journal* 92.2 (1995): 146–154. https://doi:10.14359/9765.
75. Bentur, A., & Mindess, S. (2006). Fibre reinforced cementitious composites (2nd ed.). CRC Press. https://doi.org/10.1201/9781482267747.
76. Ferraris, C. (1999). Measurement of the Rheological Properties of Cement Paste: A New Approach, Symposium of the Role of Admixtures in High Performance Concrete, Monterrey, MX, https://tsapps.nist.gov/publication/get_pdf.cfm?pub_id=860140
77. Afshinnia K, Rangaraju PR. Impact of ground glass powder on the rheological, mechanical, and durability properties of cementitious systems. *Constr Build Mater*. 2016;135:547–556. doi:10.1016/j.conbuildmat.2016.01.015.
78. Dias DP, Thaumaturgo C. Fracture toughness of geopolymeric concrete reinforced with basalt fibers. *Cem Concr Compos*. 2005;27(1):49–54. https://doi.org/10.1016/j.cemconcomp.2004.02.044.